The hippocampal intrinsic network oscillator

Yacov Fischer

Brain Research Institute, University of Zurich, CH-8057 Zurich, Switzerland

Oscillatory activity characterizes the activity of the hippocampus *in vivo*; however, the underlying mechanism remains unknown. It is also known that during oscillations the number of action potentials provided by the principal cells is surprisingly low, and it is still an open question how oscillations can emerge under such constraints. One suggestion is that the discharge activity of inhibitory cells takes this function; however, this has been found, in my previous studies, not to be the case for cholinergically mediated and intrinsically generated hippocampal oscillations. This study identifies the hippocampal intrinsic network oscillator and the interactions which underlie the concurrent expression of cholinergically mediated theta (4–15 Hz) and gamma (20–80 Hz) oscillations. A particular axonal network that involves the hippocampal associative pathway, shown to consist of axonal collaterals of CA2 and some CA3 pyramidal cells, forms the oscillator core element. It is functionally activated via two cholinergically mediated reactions. First, direct activation of CA2 and CA3 pyramidal cells to discharge. Second, enhancement of gap junction-mediated axo-axonic interactions among axons of the core element and associated axons of interneurones, which together form the full oscillator. With these two reactions it is possible to explain the rhythmicities and patterns of activity, under the condition of a low number of action potentials. The discharge of CA3 pyramidals serves mainly as a trigger, while firing by CA2 pyramidals, and to a lesser degree by CA3 pyramidals, maintains the oscillatory activity. The cholinergically mediated 2-fold increase in axonal gap junction communication between cells serves two functions: (a) creation of specific activation pathways to produce the rhythmicities and patterns, and (b) formation of a reverberatory system that extends the time during which the sparsely generated action potentials can interact in the network, thereby providing a new source of action potentials, critical for the expression of oscillatory activity.

(Resubmitted 22 September 2003; accepted after revision 22 October 2003; first published online 31 October 2003)
Corresponding author Y. Fischer: Brain Research Institute, University of Zurich, CH-8057 Zurich, Switzerland. Email: kfischer@hifo.unizh.ch

The oscillatory mode of activity is a basic operational mode of the hippocampus, and is commonly observed in EEG recording (Jung & Kornmüller, 1938; Walter, 1953). Key features of the oscillatory activity *in vivo* are as follows: (a) Concurrent expression of theta oscillations (4–15 Hz), one of the largest brain waves (Walter, 1953), and gamma oscillations (20–80 Hz) (Bragin *et al.* 1995). (b) Levels of action potential discharge are relatively low, and their frequency does not vary during hippocampal oscillations (Hirase *et al.* 2001). (c) Oscillations depend on the activity of a putative intrinsic oscillator (Kocsis *et al.* 1999). (d) Oscillatory activity depends on septal inputs (Gray, 1971; Andersen *et al.* 1979; Lee *et al.* 1994). (e) The oscillations depend on intrinsic network interactions (Buzsáki, 2002). All in all, the mechanism underlying this basic hippocampal operation remains unknown.

How oscillations are generated, maintained, synchronized and paced are central questions. Although external sources are suggested to contribute to all these processes (Buzsáki, 2002), intrinsic mechanisms may underlie them. In line with this, it has been shown that the oscillatory mode of activity can be faithfully reproduced in a hippocampal network that lacks extrinsic influences (Fischer *et al.* 1999, 2002). The network preserved in the *in vitro* system of hippocampal slice culture (Gähwiler, 1981, 1998) always adopts the oscillatory mode of activity in response to cholinergic activation, and exhibits all the above-mentioned features.

We have previously reported that the septal cholinergic input to the hippocampus is sufficient for the activation of the intrinsic network oscillator (localized in area CA3), and for the expression of concurrent theta and gamma oscillations (Fischer *et al.* 1999, 2002). Moreover,

 DOI: 10.1113/jphysiol.2003.055558

oscillations develop as a result of network interactions, while the cholinergic input has only a permissive role. Oscillations depend on the diffuse action of acetylcholine (Fischer *et al.* 1999), which is supported by the findings that the response of pyramidal cells (PCs) to cholinergic afferent activation is slow, i.e. a muscarinic EPSP of 1–3 min in duration appears within 1 s of septal afferent stimulation (Gähwiler & Brown, 1985), and that septal cholinergic afferents form free ending terminals, in addition to classical synapses, in the hippocampus (Frotscher & Léránth, 1985). Furthermore, cell classes that spontaneously discharge and the numbers of action potentials expressed by these cells are comparable to *in vivo* data (Fischer *et al.* 2002).

Generation of action potentials by the network is critical for the oscillatory activity, since it is abolished by TTX (Fischer *et al.* 2002). However, the spontaneous discharge of interneurones, the major cell class to spontaneously discharge during oscillations, is incompatible with the triggering or pacing of the oscillations (Fischer & Dürr, 2003). Therefore, identification of additional sources of action potentials becomes imperative. Natural candidates, to take over these functions are the excitatory cells. Therefore, I set out to examine the activity of individual CA1, CA2, and CA3 PCs, and dentate granule cells (DGCs), during the cholinergically mediated (methacholine; MCh; 10–20 nM) oscillatory mode of activity. Here I determine which excitatory cells discharge, and the consequences of spontaneous action potential discharge to the initiation, maintenance, synchronization, pacing and appearance of hippocampal network oscillations. I also determine whether discharge was a direct result of the cholinergic input, or was due to network interactions. Moreover, I set out to identify additional reactions that may facilitate the expression of oscillatory activity by the hippocampal network.

Methods

Slice cultures

All experiments were done according to the guidelines set forward by the Department for Veterinary Affairs of the Kanton of Zurich. Hippocampal slice cultures were prepared from 6-day-old rat pups killed by decapitation, and maintained for 3–6 weeks *in vitro* (Gähwiler *et al.* 1998).

Lesions

A lesion between fascia dentata and CA3 stratum pyramidale was made 24 or 48 h prior to recording, in a cutting medium that consisted of a normal tissue culture medium that was supplemented with 0.5 μM TTX and 10 mM $MgCl_2$.

Electrophysiological recordings

For electrophysiological recordings, cultures were transferred to a recording chamber, mounted on an upright or inverted microscope (Zeiss, Jena, Germany), and continuously superfused with warmed (32–33°C) saline containing (mM): Na^+ 145, Cl^- 149, K^+ 2.7, Ca^{2+} 2.8, Mg^{2+} 2, HCO_3^- 7.7, $H_2PO_4^-$ 0.4, glucose 5.6, and Phenol Red (10 mg l^{-1}) at pH 7.4.

Simultaneous electrophysiological recordings were obtained either from individual PCs of areas CA1 and CA3, or from individual PCs of areas CA2 and CA3, or from individual CA3 PCs and DGCs using sharp microelectrodes containing 1 M potassium methylsulphate either alone or with 2% biocytin (electrode resistance: 30–60 MΩ), as previously described (Fischer *et al.* 1999; Fischer *et al.* 2002). Only a fraction of these cell pairs were monosynaptically connected, tested by evoking an action potential (40 ms current pulse) in either of the cells, and by monitoring the postsynaptic response in the other. Recordings obtained from CA3 PCs were also used as a coherent time reference for the oscillatory activity.

Drugs

Methacholine (MCh), carbenoxolone, halothane, ammonium chloride (NH_4Cl), atropine and bicuculline were purchased from Sigma-Aldrich (Buchs, Switzerland), 1,2,3,4-tetrahydro-6-nitro-2,3-dioxo-benzo[f]quinoxaline-7-sulfonamide (NBQX), 6-cyano-7-nitroquinoxaline-2,3-dione (CNQX) and tetrodotoxin (TTX) from Tocris-Cookson (Bristol, UK), and biocytin, Lucifer yellow and micro ruby from Molecular Probes (Eugene, OR, USA). (±)-3-(2-Carboxypiperazin-4-yl)-propyl-1-phosphonic acid (CPP) was a gift from Novartis (Basel, Switzerland).

Data analysis

The analog signal was recorded on videotape at 22 kHz and digitized at 1 kHz. Analysis of oscillatory activity was based on windowed fast Fourier transform (FFT) analysis, using 500 ms windows with 50% overlap, as previously described (Fischer *et al.* 2002). Results of the windowed FFT analysis are presented in the form of spectrograms, which illustrate the Fourier analysis power spectrum (frequencies: 2–500 Hz) as a function of time, using a false colour scale to indicate the power in decibels (dB) (warm

colours represent high power and thus the dominant frequencies). Rhythmic activity in PCs was evaluated by calculating the mean of the dominant frequencies obtained from the FFT of each window (during a 10 s period of activity). For assessing gamma activity in the cells, our previously described subtraction method was used, where the slow activity content of the PCs and DGCs signals was calculated and subtracted and windowed FFT was recalculated (Fischer *et al.* 2002).

Interspike intervals were measured from signals digitized at 1 kHz. Action potential and unitary connection parameters were extracted from signals digitized at 10 kHz.

Phase analysis of CA2 PC firing was performed using the procedure described in Fischer & Dürr (2003). In brief, for each action potential in the CA2 PC (identified by a threshold method), the corresponding oscillatory cycle in the CA3 PC, its duration, and the phase relationship between the two were determined. The beginning of the corresponding oscillatory cycle (in the CA3 PC) was assigned to the onset of the population IPSP, which is zero-phase by definition. The ratio between the spike delay, i.e. the time difference between the action potential and the cycle onset, and the local cycle length (by definition 360 deg) gives the immediate phase of each action potential, which is thereafter represented in firing-phase histograms. Also here analysis was preformed on signals digitized at 1 kHz.

Calculation of the slow depolarization in CA3 and CA2 PCs (Figs 3, 5 and 6) was based on a running average of 4 s without phase shift.

Analysis was performed using Matlab (The MathWorks, Inc., Natick, MA, USA). Variability of the mean was expressed in S.D.

Dye transfer

Dye transfer properties of individual cells of the hippocampal network were measured under three experimental conditions: (a) control, (b) MCh (10–20 nM) and (c) MCh with NH_4Cl (2 mM). In each condition, a single cell (per culture) was injected with an intracellular solution containing 1 M potassium methylsulphate, 2% biocytin and 4% micro ruby. Upon penetration, the first 5 min were used to check the electrophysiological condition of the cell and to verify that only a single cell was impaled, on the basis of the fluorescent internal control micro ruby (molecular weight 3000). This was followed by 5 min exposure to control saline, or to MCh, or to MCh and NH_4Cl, and an additional 5 min of wash. Following this 15 min (in all conditions) the electrode was withdrawn, and the culture was inspected again to verify (again the fluorescent internal control micro ruby) that only the original cell was injected. For condition C, the ability to transfer Lucifer yellow (4% aqueous) was also tested. At the end of experiments, cultures were fixed with a solution containing 4% paraformaldehyde and 15% (v/v) saturated picric acid in 0.1 M phosphate buffer (PB). After fixation, biocytin injected cultures were transferred to a cryoprotective solution (30% sucrose and 12% glycerol in 0.1 M PB), frozen in dimethylbutane, and stored at –20°C until processing. For the biocytin reaction, cultures were transferred to PB (0.1 M), incubated in avidin-biotinylated horseradish peroxidase complex (ABC, 1 : 200, Vector), and transferred to Tris-buffered saline (TBS, pH 7.4). Tissue-bound peroxidase was visualized by 3,3′-diaminobenzidine 4 HCl (Sigma) as a chromogen (oxidized with H_2O_2). Following dehydration, cultures were embedded in dammar resin (Fluka, Switzerland). Lucifer yellow injected cultures were embedded in dammar resin, following fixative wash (PB) and dehydration.

Visualization of biocytin injected CA2 PCs and DGCs

Biocytin injected PCs (CA2 and CA3) and DGCs were fixed, cryoprotected, and frozen as described above. To facilitate the visualization of the axonal projections, an additional amplification step was used. Cultures were washed in PB (0.1 M, 3 × 10 min), and non-specific sites were blocked with heat inactivated horse serum (2% in PB, 1 h). Specific sites were then detected by Alexa 488-conjugated streptavidin (1 : 250, Molecular Probes, Eugene, OR, USA) (overnight 4°C, in blocking solution). Following washes and blocking (as above), cultures were incubated with a biotinylated antiavidin (1 : 1000, Vector) (overnight 4°C, in blocking solution). This was followed by incubation in avidin-biotinylated horseradish peroxidase complex (ABC, 1 : 200, Vector), visualized as above, and embedded in slowfade (Molecular Probes, Eugene, OR, USA).

Results

The role of DGCs in oscillations

Granule cells of the dentate gyrus give rise to a major excitatory pathway in the hippocampus, the mossy fibre pathway, which innervates area CA3. The involvement of DGCs and mossy fibres in hippocampal oscillations has not been characterized in hippocampal slice cultures thus far. Simultaneous intracellular recording were obtained from DGCs and CA3 PCs ($n = 7$), whose morphological identities were confirmed following biocytin injection (Fig. 1*A*). At their resting potentials, CA3 PCs

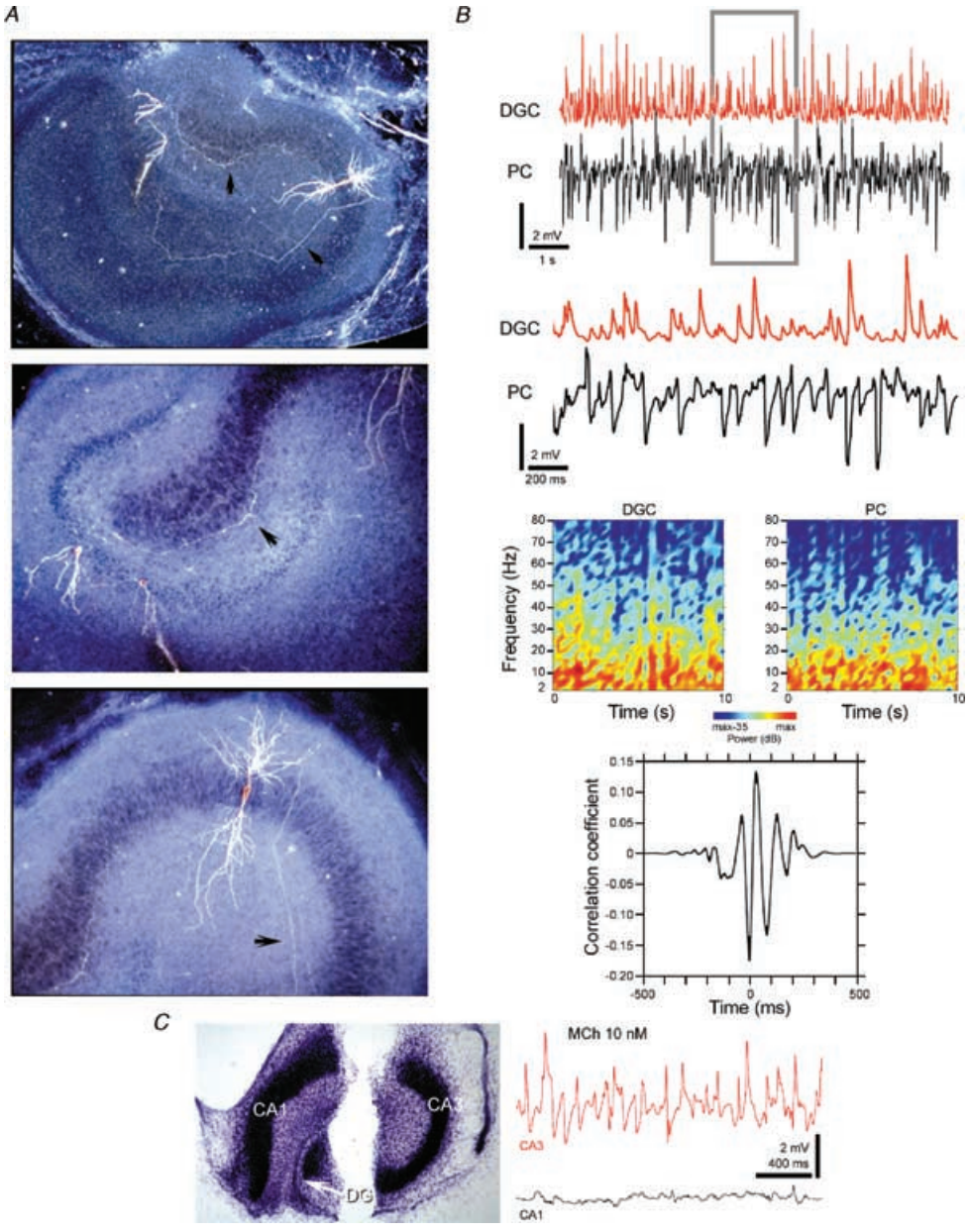

Figure 1. The dentate gyrus activity during oscillations

A, biocytin-labelled and simultaneously recorded individual DGCs and CA3 PCs. The upper panel depicts the location of the cells, their main axonal projection and dendrites. The DGC was situated in the granular layer and projected a mossy fibre toward CA3 (middle panel, the recorded DGC was the one projecting a mossy fibre, the other was accidentally filed before the experiment began). The corecorded CA3 PC was situated in the middle of str. pyramidale and its main axonal branch projected a Schaffer-collateral toward CA1 (lower panel). The recorded DGCs were characterized by a dendritic arbor that was directed toward the outer rim of the granular layer, and by an axon that formed a wiggly mossy fibre, that gave rise to putative giant and small mossy fibre terminals. Arrows mark the main axonal projections. *B*, synaptic theta oscillations were observed in the simultaneously recorded DGC and CA3 PC in response to MCh application (20 nM). Both cells exhibited ongoing rhythmic activity (upper traces, taken 5 min after the onset of oscillations); in the DGC (red) EPSPs prevailed while in the CA3 PC (black) mixed EPSP/IPSPs sequences, usually with higher weight for the IPSPs, were observed (lower traces, enlarged area is indicated by a grey square). Spectrograms depict the results of the windowed FFT analysis, and show that the activity of both cells mainly occurred in the theta band. Resting membrane potentials were –65 mV (DGC) and –59 mV (PC). Cross-correlation of the oscillatory activity in the DGC and PC depict synchrony in activity between individual cells of both regions. *C*, isolation of the dentate gyrus and area CA1 from area CA3 revealed that CA3 PCs (red) could, while CA1 PCs (black) could not, express the control oscillatory activity (MCh, 10 nM). Resting membrane potentials were –65 mV (CA1 and CA3 PCs).

(–59.7 ± 4.1 mV, $n = 7$) and DGCs (–63.4 ± 2.1 mV, $n = 7$) exhibited synaptic theta oscillations in response to MCh application (20 nM) (Fig. 1*B*). In CA3 PCs rhythmic activity was characterized by cycles consisting of population EPSP/IPSP sequences that are usually dominated by population IPSPs (see also Fischer *et al.* 1999, 2002), while in DGCs EPSPs, of duration and amplitude similar to the unitary connection from CA3 PCs (not shown), prevailed. Dominant frequencies were 7.7 ± 1.5 Hz in DGCs ($n = 6$), and 7.6 ± 1 Hz in CA3 PCs ($n = 6$) ($P > 0.05$, t test). Windowed FFT analysis also showed that activity in the gamma band was 18.5 ± 3.1 dB lower ($n = 6$) (about 100 times smaller) in DGCs. Cross-correlation analysis revealed that such patterns of activity occurred synchronously at individual cells of both regions (Fig. 1*B*). Moreover, none of the DGCs discharged during oscillations. These results indicate that the dentate gyrus plays a passive role in the generation of the oscillations. Indeed, making a lesion between fascia dentata and CA3 pyramidale (Fig. 1*C*) did not impair theta oscillations in CA3 PCs ($n = 5$), demonstrating that the dentate gyrus is not essential for intrinsically generated oscillations.

The role of CA3 PCs in oscillations

One identified source for action potentials among excitatory cells, during oscillations, are the CA3 PCs (Fischer *et al.* 1999, 2002). In general, discharge of CA3 PCs was associated with a slow transient depolarization of their membrane potential (Fig. 2). Firing itself was limited, and individual cells exhibited few action potentials during oscillatory activity (Fig. 2). Moreover, this firing preferentially occurred during the initial phase of the slow depolarization, coinciding with the onset of oscillations (Fig. 2), and subsided sharply afterwards. Overall 27% ($n = 57/206$) of CA3 PCs exhibited some form of action potential discharge during oscillations; in 84% ($n = 48/57$) firing was, and in 16% ($n = 9/57$) was not, associated with the transient membrane depolarization.

Although 45% ($n = 93/206$) of CA3 PCs exhibited the transient slow depolarization during oscillations, action potentials were observed only in 52% ($n = 48/93$) of these cells. In contrast, only 8% ($n = 9/113$) of the non-depolarizing CA3 PCs discharged. Thus, the transient slow depolarization seems to serve as the driving force for the generation of action potentials in CA3 PCs.

Whether the slow depolarization results from the direct activation of muscarinic receptors expressed by CA3 PCs or from network interactions was tested next. The slow depolarization, that accompanied the oscillatory activity (Fig. 3*A*) ($n = 93$), was abolished by atropine (0.1 μM) (Fig. 3*B*) ($n = 7/7$), and was insensitive to TTX (0.5 μM) (Fig. 3*C*) ($n = 6/6$). Furthermore, atropine (0.1 μM, $n = 22$) and TTX (0.5 μM, $n = 14$) abolished the network oscillations. Thus, the slow transient depolarization observed in CA3 PCs, resulted from the direct activation of muscarinic receptors by MCh.

The role of CA2 PCs in oscillations

In the hippocampus there exists an additional class of PCs that forms area CA2. This area can be identified following TIMM staining (Fig. 4*C*), whose reaction product defines a narrow clear region between the end of area CA3 (defined by the end of the mossy fibers projection) and the beginning of area CA1 (see also Baimbridge & Miller, 1982). I was interested in characterizing the activity of

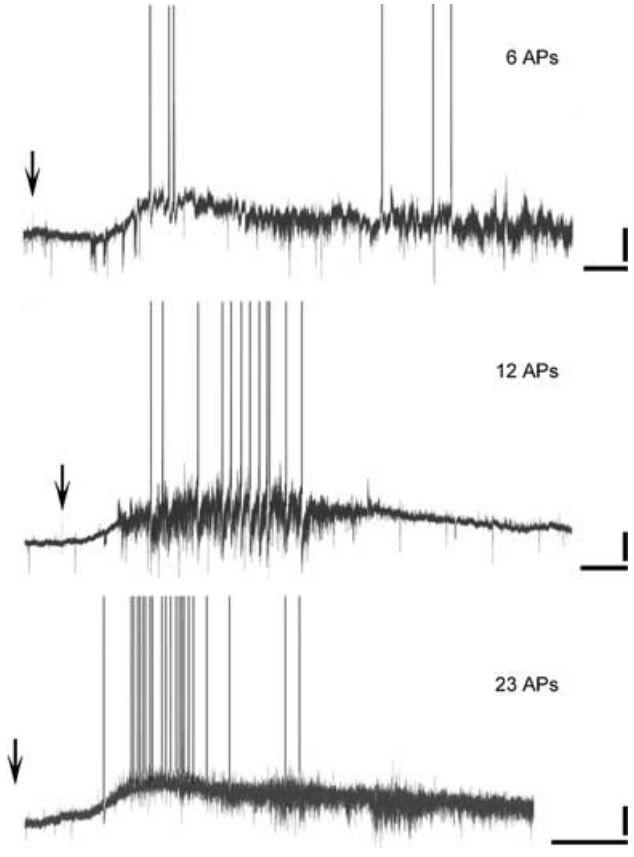

Figure 2. Action potential discharge in CA3 PCs
Action potential discharge in CA3 PCs, was observed in response to MCh application (20 nM), and was associated with the expression of a slow transient depolarization. Firing was maximal during the rising phase of the slow depolarization, and sharply decreased as the depolarization diminished. Numbers of action potential at individual cells were low, and for the 3 examples were 6, 12 and 23. Arrow: time of MCh applications, continuously superfused. Calibration: 60 s, 5 mV. Resting membrane potentials (in mV): –59 (top), –58 (middle) and –65 (bottom).

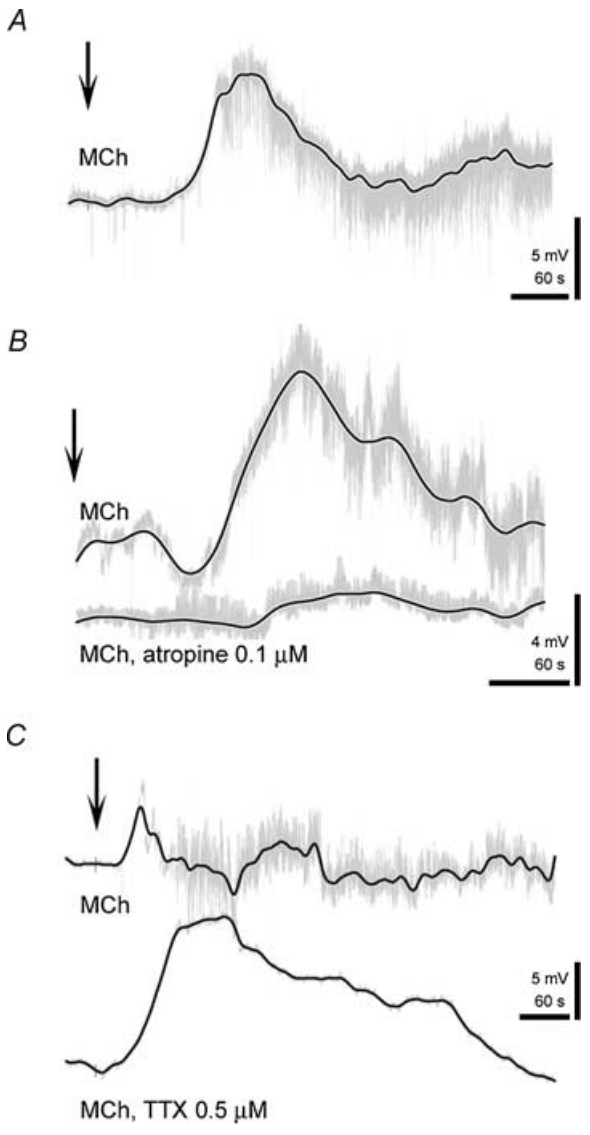

Figure 3. Transient slow membrane depolarization accompanies oscillations in CA3 PCs

A, in addition to exhibiting ongoing theta oscillations (grey line) in response to MCh application (10 nM; arrow: time of MCh applications; continuously superfused), an accompanying slow transient membrane depolarization was observed in some CA3 PCs (black line, slow response). Membrane potential rose relatively sharply, coinciding with the onset of oscillatory activity (grey), and subsided independently of the oscillatory activity (resting membrane potential: –58 mV). *B*, application of atropine (0.1 μM) abolished both the slow transient depolarization and oscillations (observed in 10 nM MCh) (resting membrane potential: –59 mV). *C*, application of TTX (0.5 μM) blocked the oscillatory activity, but not the slow transient depolarization (both mediated by 10 nM MCh) (resting membrane potential: –58 mV). Note that the MCh induced transient slow depolarization was larger in amplitude in TTX, probably due to additional non-specific interactions at control. For *B* and *C*, second application (the coapplication) was done after wash and recovery of the control MCh response.

CA2 PCs during hippocampal oscillations, and to examine whether they also serve as a source for action potentials.

In practical terms, it is relatively easy to localize CA2 PCs for recordings under visual inspection. These cells are situated after the end of CA3 pyramidale, and are identifiable by somata that are distinctively smaller than that of CA3 PCs and bigger than that of CA1 PCs. Morphological features of these PCs were revealed by the injected marker biocytin. CA2 PCs are characterized by an elongated dendritic arbor (Fig. 4*A*). The axonal arbor followed the patterns previously described (Lorente de Nó, 1934; Tamamaki *et al.* 1988), and a schematic representation is provided in Fig. 11. The axon originated in the basal dendrites and projected, in all labelled cells, a main branch toward area CA1 at stratum (str.) oriens and the alveus. Commonly, the main axon would give rise to an opposite branch directed to area CA3a, at the same strata. In some cases the main axon branched in str. oriens to send a collateral that crossed str. pyramidale in a right angle and then branched at 90 deg toward CA1 at the outer edge of str. radiatum, toward and within str. lacunosum-moleculare. Occasionally this branching would also project toward CA3a in a similar manner. However, the most extensive axonal plexus was usually observed in the vicinity of the injected cell, in areas CA2 and CA3a (see schema in Fig. 11), in str. oriens and pyramidale. Although projecting toward area CA1, CA2 PCs do not give rise to Schaffer collaterals (Fig. 1); their axon collateral that projects in the outer edge of str. radiatum is situated closer to the location of the perforant path input, over the outer apical dendrites of CA1 PCs (see also Lorente de Nó, 1934; Tamamaki *et al.* 1988).

The activity of these cells, during the cholinergically mediated oscillatory activity, was monitored in simultaneous intracellular recording form individual CA2 and CA3 PCs ($n = 17$). At their resting potentials CA2 PCs (–61.5 ± 4.8 mV, $n = 15$) and CA3 PCs (–62.4 ± 4.2 mV, $n = 16$) exhibited synaptic theta oscillations in response to MCh application (20 nM) (Fig. 4). Dominant frequencies were 7.32 ± 1.1 Hz in CA2 PCs ($n = 13$), and 7.56 ± 0.96 Hz in CA3 PCs ($n = 13$) ($P > 0.05$, t test). Windowed FFT analysis also showed that activity in the gamma band was 21.99 ± 3.12 dB lower ($n = 13$) (about 100 times smaller) in CA2 PCs, and 20.93 ± 2.49 dB lower ($n = 13$) in CA3 PCs. The rhythmic synaptic sequence observed in CA2 PCs was in between that of CA3 and CA1 PCs (Fischer *et al.* 1999; see also Fig. 7); it gradually varied from a mixed EPSP/IPSP pattern to an EPSP-only sequence (Fig. 4). The weight of IPSPs, in the sequence, was usually weaker than in the corecorded CA3 PCs (Fig. 4*B1*), with a gradual decrease in IPSPs

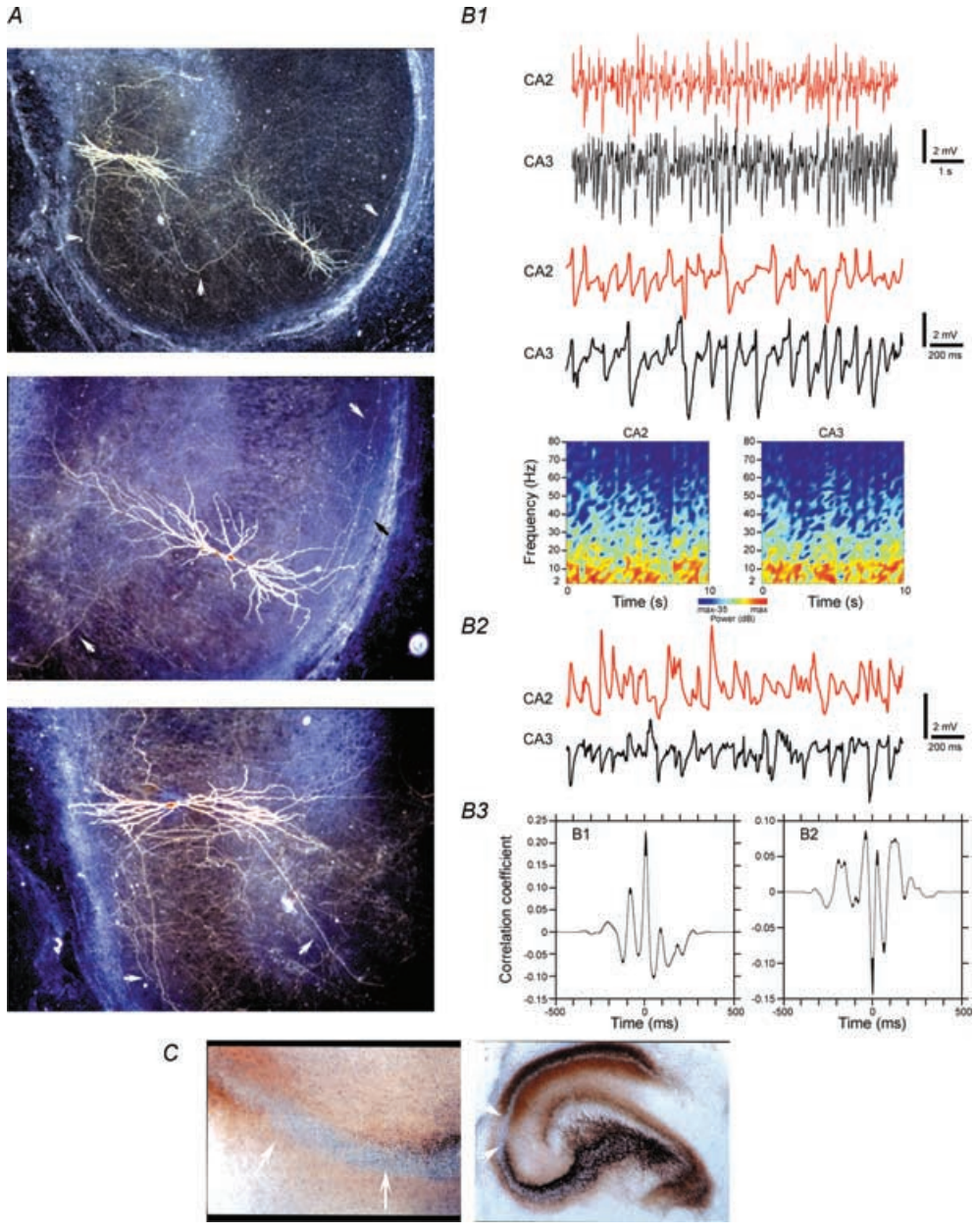

Figure 4. Activity of CA2 PCs during oscillations

A, biocytin labelled and simultaneously recorded individual CA3 and CA2 PCs. Top panel: the cell pair. Middle panel: the CA2 PC. Bottom panel: the CA3 PC. Arrows mark main axonal projections. The CA2 PC had an elongated dendritic tree. The CA2 PC emitted axonal projections toward area CA1 in str. oriens and alveus. *B1*, traces of the spontaneous intracellular activity obtained from a CA2 PC (red) and a CA3 PC (black) during MCh application (20 nM). Both cells exhibit ongoing rhythmic synaptic activity (top traces), which in a higher time base reveals a mixed sequence of population EPSPs/IPSPs (middle traces). Accompanying spectrograms depict the result of windowed FFT analysis, and demonstrate that activity in both cells was confined to the theta band. In CA2 PCs the weight of population IPSPs in the sequence is lower as compared with the corecorded CA3 PCs (*B1*, middle traces), and gradually shifted toward an EPSP dominant sequence (characteristic of CA1 PCs, see Figure 7) (*B2*, a different experiment). Such relations are evident in the cross-correlograms of these cells (*B3*), where similarity in the sequence of events (*B1*) resulted in a positive relation about the zero (*B1* cross-correlogram) and an opposite pattern (*B2*) resulted in an inverse relation about the zero (*B2* cross-correlogram). In addition the cross-correlograms show synchrony in activity between individual cells of both regions. Resting membrane potential (in mV), *B1*: –58 (CA2), –58 (CA3), *B2*: –56 (CA2), –59 (CA3). *C*, following TIMM staining, area CA2 is identifiable as a narrow, clear, region between area CA3 (characterized by a black reaction product in the mossy fibres) and CA1 (characterized by a brown reaction product in str. oriens and str. radiatum). Arrows: CA2 area limits.

toward an EPSP dominated sequence (Fig. 4*B2*). For the cell pair depicted in Fig. 4*B1*, the inhibitory input to the CA3 PC, during the 10-s period of analysed oscillatory activity, consisted of 89 IPSPs (2.30 ± 1.24 mV), while that to the CA2 PC contained 64 IPSPs (1.43 ± 0.73 mV) ($P < 0.05$, t test, for amplitude). For the cell pair depicted in Fig. 4*B2*, and in contrast to the oscillatory sequence of the CA3 PC, where 92 IPSPs (0.99 ± 0.55 mV) were observed during 10 s of analysed oscillatory activity, that of the CA2 PC consisted mainly of EPSPs (92 events, 1.77 ± 0.85 mV). Only 15 IPSPs (0.94 ± 0.32 mV) were observed at the same period in the CA2 PC. These EPSPs are likely to result from synchronized synaptic inputs from CA3 PCs, as action potential stimulation of CA3 PCs produced a unitary EPSP of 1.07 ± 0.45 mV (latency: 4.7 ± 1.67 ms) in the corecorded CA2 PCs ($n = 12/17$) and as CA3 PCs spontaneously discharged during oscillations. An opposite connection was observed in two cases. Cross-correlation analysis showed that such patterns of activity occurred synchronously at individual cells of both regions (Fig. 4*B3*). The rhythmic patterns observed in CA2 PCs correspond to the fact that this region is situated at the border of influence of discharging CA3 interneurones, cells that in their innervation largely respect the subfield boundaries (Freund & Buzsáki, 1996).

In 9 of the 17 CA2 PCs a slow sustained depolarization accompanied the oscillatory activity (Fig. 5*A*). The slow depolarization developed more gradually than in CA3 PCs (Fig. 6), was sustained and was temporally modulated (about every 60 s, Fig. 5*A*). As with CA3 PCs, the sustained temporally modulated depolarization was insensitive to TTX (0.5 μM, $n = 5$).

In eight out of these nine CA2 PCs, action potential firing accompanied the slow depolarization. In five cells, discharge was extensive and lasted for minutes; median firing rates were between 0.56 and 3.7 Hz (Fig. 5*B*). Analysis of the spontaneous discharge in those five CA2 PCs showed that the sequence in which action potentials occurred was structured to exhibit acceleration in the interspike intervals (Fig. 5*C*), corresponding to the temporal modulation of the slow depolarization (Fig. 5*B*). Instantaneous frequencies of action potentials varied between 0.01 and 100 Hz (Fig. 5*C*). Moreover, instantaneous firing frequencies exhibited, in the log domain, a unimodal normal distribution whose peak appeared in the theta band (Fig. 5*C*).

The temporal relationship between the spontaneous discharge of CA2 PCs and the immediately relevant theta cycles in the corecorded CA3 PCs was determined ($n = 5$). In contrast to spontaneous firing in CA3 interneurones (Fischer & Dürr, 2003), discharge in all five CA2 PCs was not temporally structured to occur at specific and limited portions of the oscillatory cycle. An apparent modulation in the firing phase histogram (Fig. 5*C*) was not a consistent feature, and in the five experiments somewhat elevated discharge at 30, 80, –80, 10 and 50 deg accompanied consistent contributions at all phases of the cycle. Therefore, firing occurred almost equally at all portions of the oscillatory cycle, thus providing a temporally uniform source of action potentials (Fig. 5*C*).

Additional reactions

Thus, the patterns of action potential firing, in the excitatory cells, do not lend themselves to a 'simple' explanation of the oscillatory activity, as their numbers are low (see Discussion) and as they are temporally uncorrelated with the oscillatory cycles. Therefore additional interactions must exist in order to translate the kernel of action potentials, i.e. the pool of all PC-generated, action potentials available at any given time, into the oscillatory patterns. Moreover, such interactions should occur in a manner that would provide the 'clock' function, i.e. the property of the network to synchronize and pace the rhythmic synaptic activities, such that theta and gamma oscillations of the patterns and properties found would emerge (given the action potential kernel constraints). I therefore decided to test whether it is possible to identify interactions between the discharging cells which may facilitate the expression of oscillatory activity, in particular the possibility that axo-axonal communication, mediated by gap junctions, may provide this function.

Additional reactions: pharmacology. The first approach used was pharmacological. Several compounds, such as halothane, octanol and carbenoxolone, are reported to block gap junction communication (Johnston *et al.* 1980; Leslie *et al.* 1998), and to diminish oscillatory activity (Draguhn *et al.* 1998; Traub *et al.* 2000). The effect of halothane and carbenoxolone on the cholinergically mediated oscillations was evaluated in simultaneously recorded CA3 and CA1 PCs. Application of halothane (5 mM, $n = 9$) strongly hyperpolarized the membrane potential of the cells by about 20 mV. The hyperpolarization developed gradually, over a couple of minutes, and prevented the expression of oscillatory activity. Likewise carbenoxolone application (100 μM, $n = 2$; 200 μM, $n = 6$; 20 μM, $n = 4$) resulted in slowly developing hyperpolarization. Due to these 'non-specific' effects, such compounds cannot be used for

the investigation of the involvement of gap junction communication in the oscillatory response.

Another chemical manipulation designed to target gap junction communication during oscillations was to use the alkalizing agent ammonium chloride (NH_4Cl). Gap junction opening is suggested to be enhanced during the alkalization of the cytosol by NH_4Cl, and upon removal of NH_4Cl to be consequently suppressed, due to acidification of the cytosol and the closure of gap junctions (Spray *et al.* 1981; Thomas, 1984; Draguhn *et al.* 1998). At the commonly used concentration of 10 mM ($n = 5$), and at 5 mM ($n = 2$), NH_4Cl was found to have deleterious effects on CA1 and CA3 PCs and caused instability to the cells and their ultimate death. Therefore the concentration of NH_4Cl was reduced to 2 mM, a concentration in which no deleterious effects on PCs of areas CA1 and CA3 were observed. In six simultaneously recorded CA1 and CA3 PCs (Fig. 7) the effects of NH_4Cl (2 mM) application

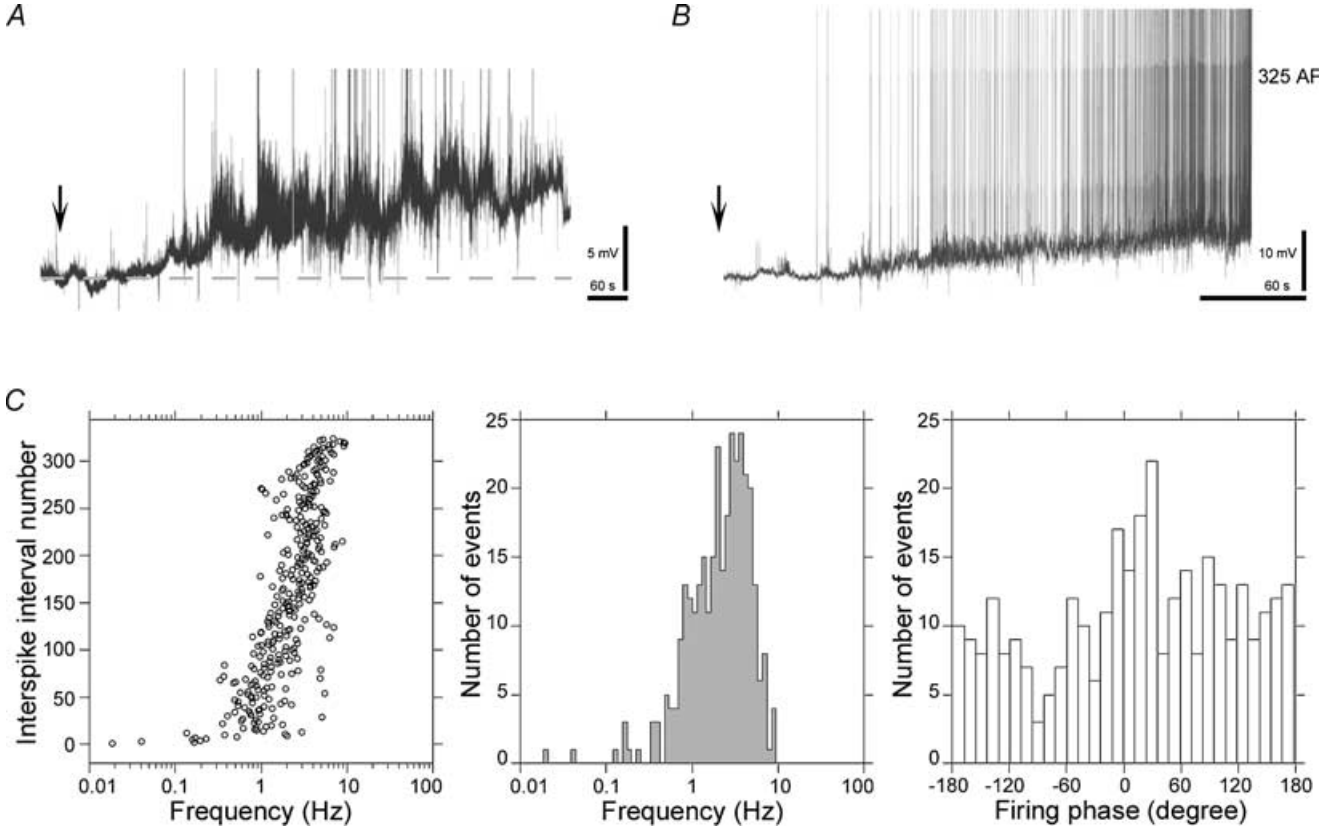

Figure 5. A slow, gradually developing, time-modulated, sustained depolarization underlies the discharge activity of CA2 PCs

A, a slow, gradually developing, time-modulated, sustained depolarization was observed in CA2 PCs during MCh application (20 nM; arrow: time of MCh applications; continuously superfused). Expression of this depolarization was due to activation of intrinsic cholinergic receptors, and occurred at a slower time course as compared to CA3 PCs (Figs 2, 3 and 6). The depolarization was temporally modulated about every 60 s. *B*, in some CA2 PCs this depolarization was accompanied by sustained action potential firing, where 325 action potentials were observed during 300 s of oscillatory activity. Firing followed the temporal modulation (about every 60 s) of the slow membrane depolarization. Arrows: time of MCh application (continuously superfused). *C*, the properties of spontaneous discharge in the CA2 PC depicted in *B*. Left: the temporal sequence of interspike intervals exhibited a pattern of acceleration, which followed the slow depolarization and its temporal modulation. This is seen as diagonally rising groups of overlapping circles, in the interspike interval sequence, indicative of an increase in the instantaneous firing rates. Middle: instantaneous firing frequency histogram shows a unimodal distribution in the log domain with a median rate of 2.38 Hz. Right: the phase relationship of spontaneous discharge in the CA2 PC to the oscillatory (theta) cycles in the corecorded CA3 PC. Firing, in the phase domain, was largely not correlated with the oscillatory cycle, and occurred almost equally at all portions of the oscillatory cycle, giving a uniform firing source of 10.8 ± 4 action potentials (for the analysed period), although the apparent increase at 30 deg and decrease at –80 deg. Resting membrane potentials: –58 mV (*A*), –56 mV (*B*).

were examined after confirming the control oscillatory theta response (MCh, 20 nM) (Fig. 7*B*) (Fischer *et al.* 1999). Application of NH_4Cl, in the control saline, had no apparent effect on the basal activity of the recorded cells (for a period of 7–10 min), nor did it elicit oscillatory activity ($n = 6$) (Fig. 7*C*). Adding MCh in the presence of NH_4Cl again elicited oscillatory activity, but the weight of IPSPs in the rhythmic sequence of CA3 PCs decreased and the weight of EPSPs increased (Fig. 7*D*). At the same time, the amplitude of the population EPSP theta sequence in the corecorded CA1 PCs increased, in a time-variable manner, 2- to 4-fold (Fig. 7*D*). Both effects, on the oscillatory activity of CA3 and CA1 PCs, were immediately apparent upon expression of oscillations by the network. At this point NH_4Cl was removed, still in the presence of MCh. This resulted in the rapid (within 2 min) blockade of oscillatory activity in both cells (Fig. 7*E*). Such blockade of the cholinergically mediated oscillatory activity was never observed under control conditions. Reapplication of MCh, after wash, elicited the control theta oscillations in both cells (Fig. 7*F*), which subsided following 5–10 min wash (Fig. 7*G*). Such effects are in accordance with the time course of alkalization, acidification, and recovery by NH_4Cl, where cells maintain an alkalized state for the duration of NH_4Cl application used here, acidify almost immediately (about 1 min) upon removal of NH_4Cl and recover (due to homeostasis) in about 15 min (Thomas, 1984). Moreover, none of the CA1 PCs used in this experiment, or others, discharged during oscillations (author's unpublished results, $n = 108$). These results indicate that the opening and closure of gap junctions has immediate and profound effects on the oscillatory activity.

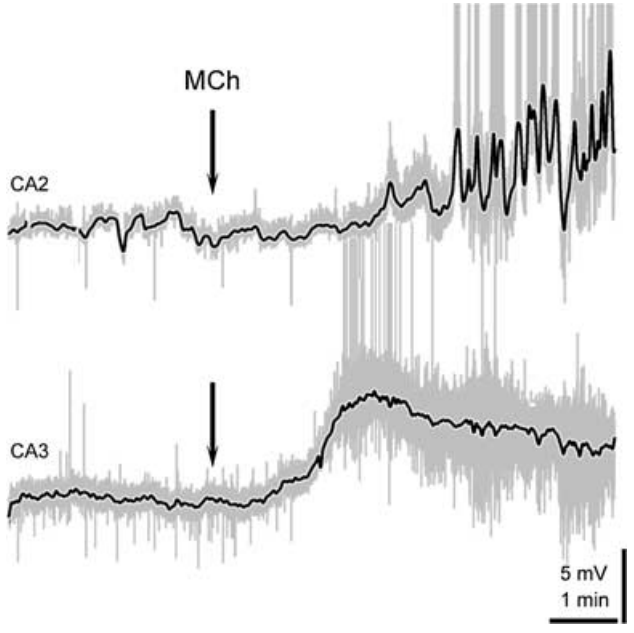

Figure 6. Relative time course of slow membrane depolarizations in CA2 and CA3 PCs
Simultaneous recording form a CA2 (top) and CA3 (bottom) PCs. Prior to MCh application (20 nM), cells were quiescent and their membrane potential fluctuated about the resting potential (CA2: –58 mV, CA3: –65 mV). Upon application of MCh (arrow: time of MCh applications; continuously superfused) the CA3 PC expressed slow transient depolarization, and the CA2 PC slow gradually developing sustained depolarization, with a slower onset compared to that of the CA3 PC (black). Both cells expresses sustained synaptic oscillations (grey) whose onset coincided with the peak of the depolarization in the CA3 PC (see also Figs 2 and 3), and discharged. The CA3 PC mainly discharged at the onset of the oscillatory activity, and the CA2 PC at later time points (action potentials are truncated).

Additional reactions: dye transfer. The second approach used was to test whether the gap junction-mediated interactions between cells could be visualized by monitoring the dye transfer properties of a single CA3 cell (per culture) under various conditions. Experiments were preformed under three conditions: control ($n = 26$), MCh (20 nM) ($n = 34$), and coapplication of MCh (20 nM) and NH_4Cl (2 mM) ($n = 18$). Estimation of the dye transfer rates was based on the visualization of the marker biocytin, coinjected with micro ruby acting as an internal control (a combination permissive for electrophysiological measurements). Results are summarized in histograms (Fig. 8) that depict the number of additional cells in which biocytin reaction product was observed. At control, in 13 of the 26 cultures there was no dye transfer, while in 12 cultures transfer to one to three additional cells was detected, and in one case to eight additional cells, giving an average rate of 1.11 ± 1.7 cells. During MCh application only 5 of the 34 cultures did not exhibit dye transfer, and in the remaining 29 cultures transfer to one to eight additional cells was detected, resulting in an average rate of 2.26 ± 2.3 cells. When MCh and NH_4Cl were coapplied, only in a single culture dye transfer was not observed, while in the other 17 cultures transfer to 1–20 additional cells was measured, resulting in an average rate of 7 ± 5.8 cells. Dye transfer rates in each condition were significantly different ($P < 0.05$, t test). With the exception of two cases, in which 20 adjacent cells were revealed after application of MCh and NH_4Cl, dye transfer was characterized by specific labelling of well defined separate cells that were not immediately adjacent to the injected cell (Figs 8 and 9), including PCs and interneurones. Furthermore, no dye transfer was detected when the marker Lucifer yellow was used for MCh and NH_4Cl coapplication ($n = 12$, not

shown), a dye that in contrast to biocytin does not label the axonal compartment, but mainly labels the somatic and dendritic compartments, of the injected cells (Buhl & Lübke, 1989), thus indicating that the dye transfer reaction occurs in the axonal compartment of the cells. Thus, MCh specifically triggered the axonal coupling via gap junctions.

Additional reactions: spikelets. The third approach was to see whether spikelets, suggested to originate by gap junction communication between cells (Traub *et al.* 1999; Traub & Bibbig, 2000), could be resolved in the oscillatory activity of different cells. Both in CA3 (48%, $n = 32/67$) and CA2 (47%, $n = 8/17$) PCs as well as in CA3 interneurones (64%, $n = 28/44$), i.e. the cell classes that spontaneously discharge during oscillatory activity (current results and Fischer *et al.* 2002), spikelets could be observed in the oscillatory sequence (Fig. 10), although they did not dominate the rhythmic synaptic sequence of the cells. It should be noted the rates of spikelets occurrence in the cell classes are underestimated, and can be taken only as a lower estimation (see Discussion). Spikelets were commonly characterized by a brief, as compared to the simultaneous synaptic activity, upward and downward deflection of the membrane potential. Such waveforms are indicative of an axonal origin (Traub *et al.* 1999; Traub &

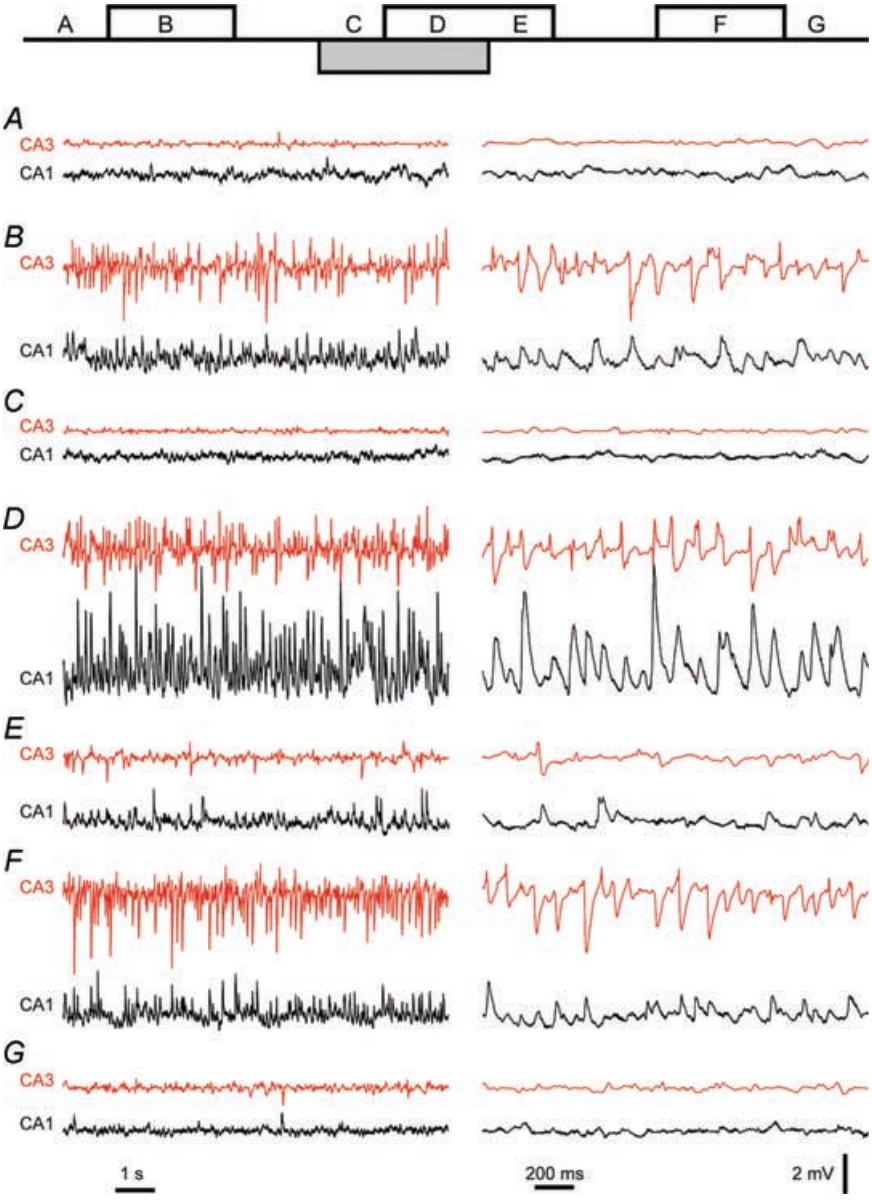

Figure 7. Effects of cytosol alkalization and acidification on oscillations
The effects of NH_4Cl on cholinergically mediated network oscillations in areas CA3 and CA1 were examined in simultaneous intracellular recording from individual CA1 and CA3 PCs. Top diagram: the experimental protocol; letters indicate the different stages of the experiment and representative traces appear below (left traces: 10 s; right traces: 2 s). Open boxes: MCh application (20 nM). Grey box: NH_4Cl application (2 mM). *A*, in control saline both cells were quiescent. *B*, control oscillatory response was observed upon MCh application. The CA3 PC exhibited a mixed EPSP/IPSP theta sequence, with a high weight for the IPSPs. At the same time the, CA1 PC exhibited an EPSP theta sequence. *C*, NH_4Cl, on its own, had no effect on the cells. *D*, application of MCh, in the presence of NH_4Cl, again mediated the oscillatory response. However, the weight of IPSPs, in the CA3 PC theta sequence, decreased, and the weight of EPSPs increased. At the same time, the amplitude of the population EPSPs in the CA1 PC theta sequence increased 2- to 4-fold. *E*, removal of NH_4Cl, still in the presence of MCh, blocked oscillatory activity within 2 min. *F*, control oscillatory response was regained after wash. *G*, cells recovered from oscillatory activity after 5–10 min wash. Resting membrane potentials: –60 mV (CA3), –67 (CA1).

Bibbig, 2000), reflect the active propagation of transmitted action potentials, and suggest that gap junction-mediated axo-axonic communication occurred.

The intrinsic oscillator

Lastly, I report of experiments showing that the intrinsic oscillator, in the terms described in the Summary and Discussion, and illustrated in Fig. 11, is functional under conditions where fast excitatory and inhibitory transmission are eliminated from the network. Under such conditions, the core element is expected to remain active through the suggested mechanisms of (a) the creation of axonal activation pathways in the axonal network of the intrinsic oscillator and (b) the formation of a reverberatory system that maintains a critical number of

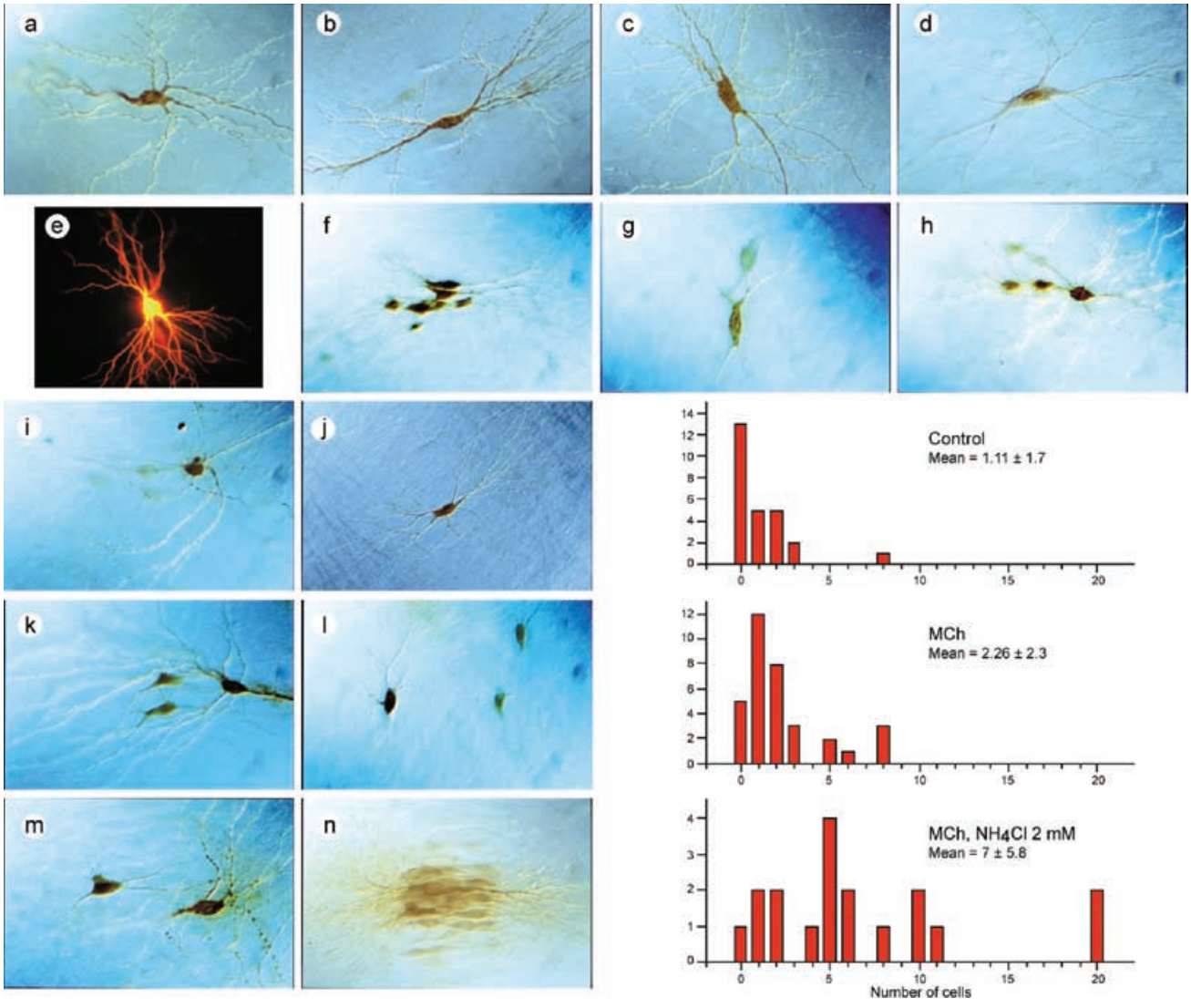

Figure 8. Dye transfer properties of the hippocampal network
Dye transfer properties were determined under 3 conditions: control (*A–D*) (26 cultures), MCh application (20 nM) (*F–J*) (34 cultures) and MCh (20 nM) and NH_4Cl (2 mM) coapplication (*K–N*) (18 cultures). Results are summarized in accompanying histograms, which depict the number of additional biocytin labelled cells. At each condition, a single cell per culture was coinjected with biocytin and micro ruby (as internal control, *E*). At control, in most cases the biocytin reaction product reveals only the injected cell. With MCh dye transfer to several, well-defined and separate, cells were observed, including PCs and interneurones. Upon coapplication of MCh and NH_4Cl, higher rates of dye transfer were observed, with similar properties as in MCh application, except for 2 cases where a cluster of about 20 cells is revealed (*N*). Average dye transfer rates, for the different conditions, accompany each histogram.

action potentials in the core element. In three experiments clear effects were observed. First, the response of individual CA3 PCs (five cells) to application of MCh (20 nM) was examined, to which the cells exhibited the control oscillatory response (Fig. 12). From this activated state of the network, and still in the presence of MCh, fast glutamatergic (CPP 10 μM, CNQX 20 μM or NBQX 20 μM) and GABAergic (bicuculline 20 μM) transmission were blocked. As all synaptic contributions are eliminated, traces depict the residual activity, which consisted of spikelets (indicative of axonal origin) (Fig. 12). These spikelets were found to be sensitive to TTX (0.5 μM), which led to the almost full elimination of the residual activity (Fig. 12). Thus it can be concluded that the residual activity depends on the generation and transmission of TTX-sensitive action potentials and spikelets in the axonal network that forms the intrinsic oscillator. In an additional four similar experiments spikelets were not observed. This may have been due either to the lack of functional coupling between the recorded cells and the core element, or to functional coupling that occurs at an electrical distance that is not detectible by the recording method. Moreover, such patterns of spikelets do not demonstrate the rhythmicity itself, although they may provide an estimate to the range in which individual cells could contribute to the oscillatory pattern by the new mechanism, and they suggest that single cells are unlikely to pace the network.

Discussion

The results identify the hippcampal intrinsic oscillator, and the cholinergically mediated reactions that lead to its functional activation and consequent development

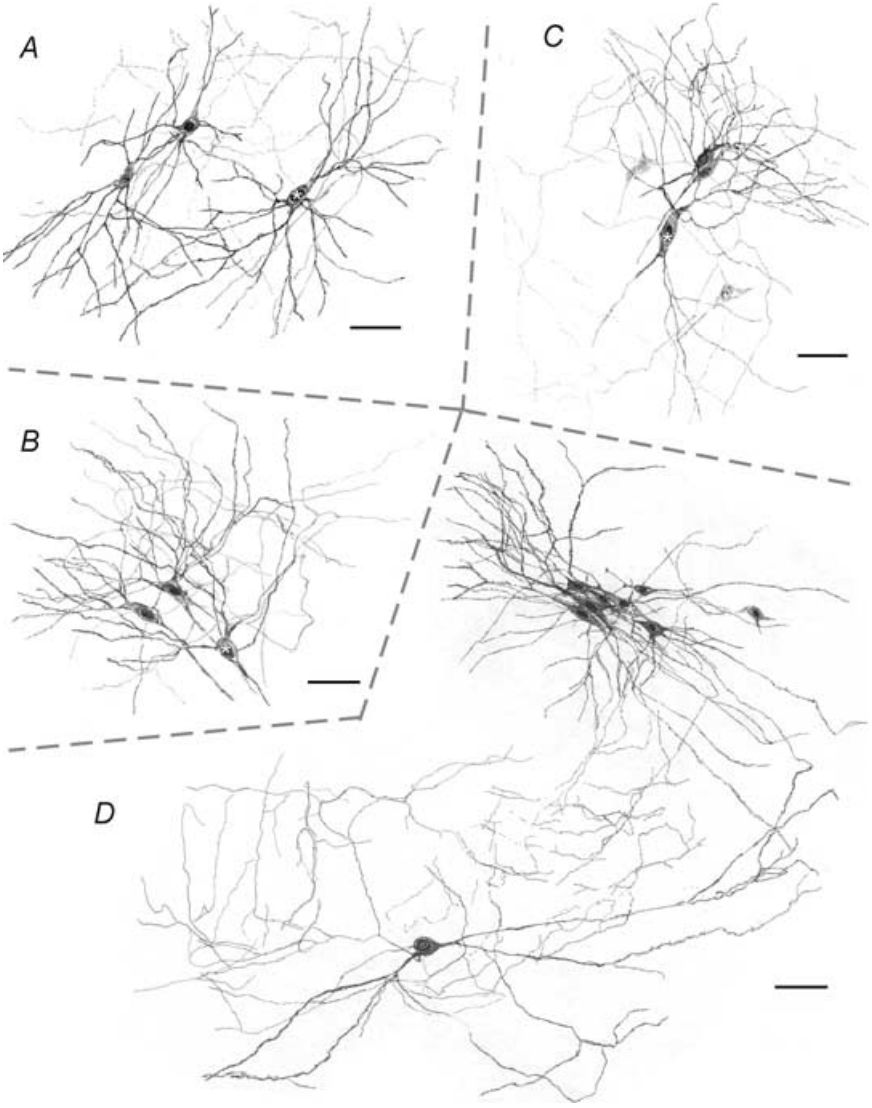

Figure 9. Camera lucida drawing of the dye transfer reaction
Camera lucida drawings of the dye transfer reaction for MCh application, alone (*C* and *D*) or with NH_4Cl (*A* and *B*). The culture drawn in panel *A* is the same one depicted in panel *I* of Fig. 8 (*B*, *C* and *D* are, respectively, *K*, *G* and *F* in Fig. 8). Asterisks mark injected cells. Calibration: 50 μm. *A*, biocytin reaction product was found in two additional PCs, which are not immediately adjacent to the injected cell. *B*, two additional PCs are revealed following the biocytin reaction. *C*, four additional cells are revealed; two are labelled stronger and two weaker. *D*, eight additional cells are revealed by biocytin, including a distant basket cell. In all cases, an elaborated axonal network, in the vicinity of the cells, was observed.

of oscillatory activity in the hippocampus. Oscillatory activity is an emergent property of the hippocampal network. Cholinergic input leads to the activation of the intrinsic oscillator core element, the hippocampal associative pathway, by evoking action potential discharge in CA2 and CA3 PCs, and by enhancing gap junction-mediated axo-axonic interactions in the core element. Together with consequent activation of interneurones, the full oscillator is formed. Hereafter, the discussion will address how oscillations are initiated, maintained, synchronized and paced, and how specific patterns are adapted.

The action potential kernel during oscillations

Generation of action potentials is critical for the expression of oscillatory activity by the hippocampal network, as their elimination (by TTX) abolishes the oscillatory activity. Therefore it was necessary to identify the cells that are spontaneously discharging, to determine whether the discharge was a direct result of cholinergic activation, and to establish the relation of the discharge to the oscillatory activity.

Three major cell classes are identified as spontaneously discharging during cholinergically mediated oscillatory activity, CA3 and CA2 PCs and CA3 interneurones.

CA3 PC discharge was consistent with participation in both the triggering and maintenance of oscillatory activity. However, discharge of individual cells was scarce, such that the precise timing of their action potential in relation to the oscillatory cycles was not determinable, and was observed in about 25% of the population. Given the fraction of discharging cells (25%), the population size (5000 cells) and the firing rate (0.03 Hz, Fischer *et al.* 2002), it is calculated that CA3 PCs contribute three to four action potentials per theta cycle in total. Discharge resulted from a cholinergically induced slow transient membrane depolarization, and was correlated and associated with its waveform. Nevertheless, expression of the slow transient

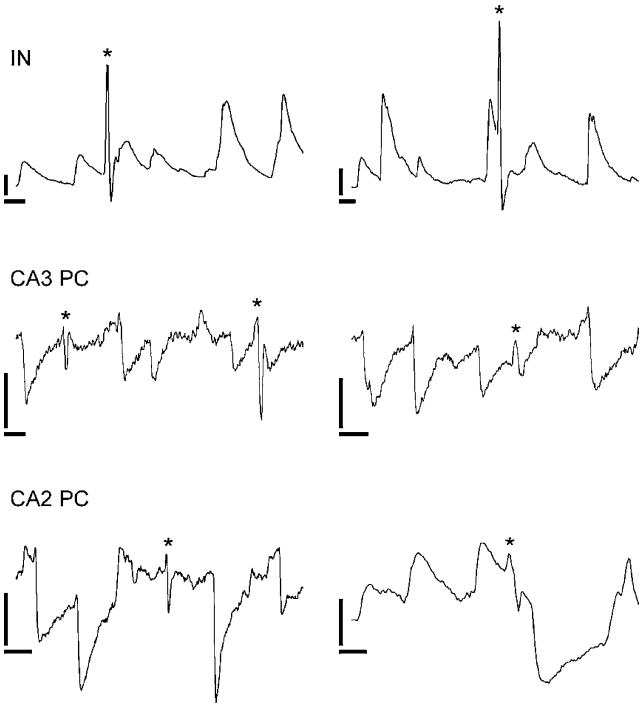

Figure 10. Spikelets are observed during oscillations
All cell classes that spontaneously discharge during oscillations exhibit spikelets. Examples are provided for interneurones (top), CA3 PCs (middle) and CA2 PCs (bottom). Asterisks mark the spikelets. Spikelets are brief in comparison to the synaptic oscillatory activity, with typical appearance of an upward and downward deflection in the membrane potential. Their occurrence was not directly affected by the synaptic events. Not every oscillating cell expresses spikelets. Calibration: vertical: 2 mV; horizontal: interneurone (IN): 20 ms; CA3 PC: 50 ms; CA2 PC: 50 ms (left), 20 ms (right).

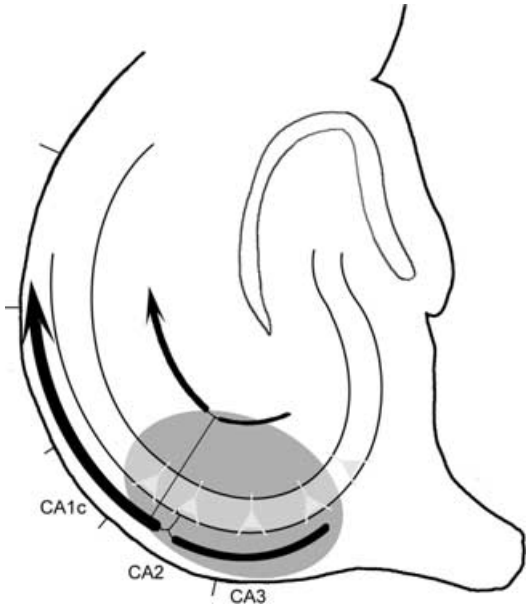

Figure 11. The core element of the intrinsic network oscillator
Schematic representation of the core element of the intrinsic network oscillator. The grey ellipsoid depicts the hippocampal associative pathway, originally described by Lorente de Nó (1934), and is formed by an elaborated axonal network of excitatory cells that discharge during oscillations. Both CA2 and CA3 PCs contribute to the oscillator core element (the associative pathway). A schematic representation of the main axonal projection of a CA2 PC is illustrated (line thickness represent the rate of occurrence); however, the main axonal plexus is within the region of the oscillator. CA3 PCs also contribute to the oscillator, and in some cells the main axonal plexus is also situated in the oscillator. According to previous anatomical studies, there is a gradient of contributing CA3 PCs; the closer the cell is to area CA2 the more likely it is to contribute to the oscillator.

depolarization translated to firing only in about 50% of the cases. Moreover, some CA3 PCs discharged at their resting membrane potential, without the activation of this process. Why only a fraction of the CA3 pyramidal cells transiently depolarize, and only a fraction of those discharge, may be due in part to differences in (a) the receptor subtypes and/or subunit composition, (b) the apparent affinity of the muscarinic receptors, or (c) the transduction mechanism underlying the expression of the slow transient depolarization.

CA2 PC discharge was consistent with being involved in the maintenance of oscillatory activity. In about 30% of the population relatively extensive firing was observed, and although discharge was mainly in the theta band instantaneous firing frequencies spanned a large range (0.01–100 Hz). Moreover, firing was largely not correlated with the oscillatory cycles. Thus, CA2 PCs produced a uniform source of action potentials. Discharge resulted from a cholinergically induced gradually developing sustained depolarization, and followed its time course. Nevertheless, area CA2 is limited in length (100–150 μm; Swanson *et al.* 1978) and the total number of action potentials produced is relatively low. Assuming a population size of 300 cells, it is estimated, on the basis of the cell fraction that discharges and the range of median firing rates, that CA2 PCs contribute a total of 5–30 action potentials per theta cycle.

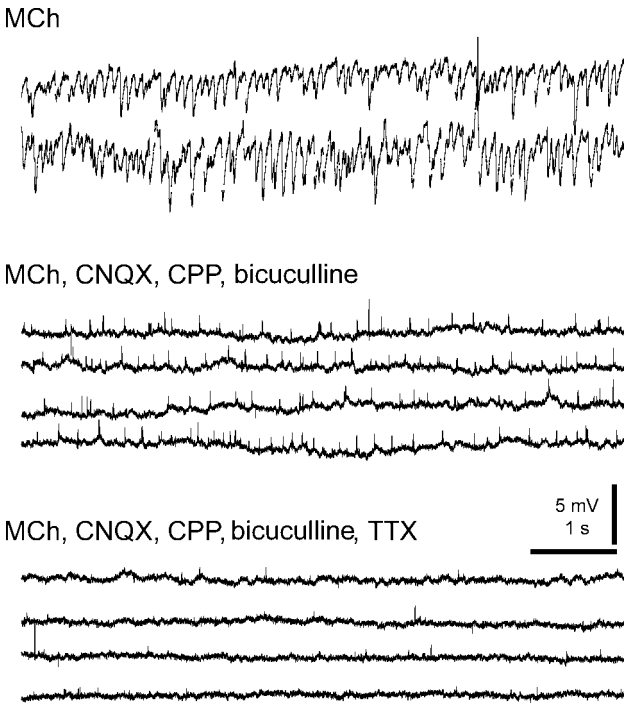

Figure 12. The oscillator is functionally active irrespective of fast synaptic interactions in the network

Intracellular recordings from a CA3 PC were preformed at 3 different conditions with respect to the cholinergic input (the enabling agent). Control oscillatory response was observed in the CA3 PC when the enabling agent (MCh, 20 nM) was applied in the intact hippocampal network. When the network was still exposed to the enabling signal (MCh), but all fast synaptic transmission was eliminated (CNQX, 20 μM; CPP, 10 μM, bicuculline, 20 μM), the synaptic oscillatory pattern was no longer observed; however, not all activity in the network was eliminated, and residual activity, which consisted of spikelets, remained. However, when subsequently TTX-sensitive action potentials were eliminated (TTX, 0.5 μM), spikelets were inhibited and the network became quiet. This result shows that the axonal pathways, and the reverberatory system, remained active to circulate spikelets, i.e. the core element was active.

CA3 interneurones form the largest source of action potentials in the hippocampal network during oscillations, where basket, O-LM, bistratified, str. lucidum-specific and multisubfield cells (Fischer *et al.* 2002) provide a total of 10–80 action potentials per theta cycle (Fischer & Dürr, 2003). Their discharge was found to determine the apparent oscillatory sequence of CA3 PCs, and to dynamically regulate the network interactions (Fischer & Dürr, 2003). However, the discharge of interneurones did not result from direct cholinergic activation, the duration of individual interneurones' synaptic output did not determine the frequencies of oscillatory activity, the time at which action potentials occurred was incompatible with pacing or triggering of the oscillations, and their firing activity was governed by non-interneuronal network interactions (Fischer & Dürr, 2003). Finally, it is hard to explain how interneurone discharge develops, as they do not depolarize during oscillations (Fischer *et al.* 2002; Fischer & Dürr, 2003).

These properties of discharge mean that the firing of CA2 and CA3 PCs is critical for the expression of oscillatory activity. However, this also illustrates the difficulty in explaining the oscillatory activity in conventional terms: a cell fires an action potential that travels along its axon to produce release of transmitter that produces an oscillatory cycle. The difficulty appears in several critical aspects. (a) Even if we are to assume a connectivity rate of 50% in area CA3 and of 10–20% from area CA3 to area CA1, then there are not enough action potentials to produce just a simple sequence of consecutive synaptic events. (b) The excitatory oscillatory patterns are based on population event, so it becomes even more difficult to explain such output, not to mention the issue of synchronization, with the number of action potentials generated by principal cells. (c) Principal cell discharge does not explain at all how discharge in interneurones originates and how IPSPs are generated.

How to proceed?

The key issue is how the network utilizes the action potentials generated by the excitatory cells for the expression of synchronous and coherent oscillatory activity. As excitatory action potentials were scarce and/or not correlated with the oscillatory cycle, additional interactions are required. The cholinergically mediated and newly identified reaction of facilitating axo-axonic interactions, by enhancing gap junction opening, may serve this function. Several lines of evidence supported this. Dye transfer experiments indicated that the site of interaction was axonic. Moreover, spikelets, with a waveform indicative of axonic origin (Traub *et al.* 1999; Traub & Bibbig, 2000), were observed in CA2 and CA3 PCs and in CA3 interneurones during oscillations. Furthermore, alkalization and acidification of the cytosol, considered to target gap junctions (Spray *et al.* 1981; Thomas, 1984; Draguhn *et al.* 1998), effectively influenced the oscillatory activity. Thus, gap junctions are the likely candidates to mediate these axo-axonic interactions.

The role of gap junctions in oscillations

How does enhancement of gap junction opening in the axonal network lead to the expression of coherent and synchronous oscillatory activity? Since the oscillatory patterns are based on synaptic sequences, oscillations depend on the creation of activation pathways that would produce them. A 'simple' explanation is that the chance of creating consecutive activation sequences is enhanced by the opening of axo-axonic gap junctions. As a result, action potentials are transmitted to axons of inhibitory and excitatory cells that otherwise would not reach the discharge threshold, thereby allowing the creation of activation sequences of specific synaptic patterns. By coordinating the opening and closing of these transmission lines, coherent and synchronous patterns are achieved.

To ensure reliability in this reaction, only a fraction of the available gap junctions are activated at any given time during oscillations. Dye transfer experiments showed an average opening of 2.26 gap junctions per cell during oscillations (assuming a 1-to-1 ratio of coupling and molecules), out of seven functionally available gap junctions per cell, which doubles the basal level of 1.11 gap junctions per cell. These experimental values (1.11 and 2.26) correspond to (a) the percolation limit, i.e. the theoretical number of functional gap junctions per cell above which a significant effect on the network activity can be expected, and (b) the theoretical estimation of 2.5 functional gap junctions per axon required for the expression of hippocampal oscillatory activity (Traub *et al.* 1999, 2000; Traub & Bibbig, 2000).

The second functional consequence of gap junction opening, which promotes the expression of oscillatory activity, is the creation of a reverberatory system. As a result of the opening of axonal pathways between cells, and depending on the probability of maintaining an activation pathway, action potentials can 'circulate' in the axonal network and thus form a reverberatory system. The benefit of such a system is that the rarely generated action potentials can extend their normal time span, thereby, ensuring a critical number of available action potentials, and increasing the chance to express synchronous and coherent activation sequences.

Both functions of gap junction opening, i.e. the activation pathways and the reverberatory system, create a new source of action potentials in the network, in addition to the somatic one.

The core element underlying oscillations

To be operative the anatomical structure of the network must support these functions. A special anatomical structure, the hippocampal associative pathway (Lorente de Nó, 1934; Swanson *et al.* 1978), is formed by axons of discharging PCs. The elaborate plexus formed in str. oriens, pyramidale and radiatum of areas CA2 and CA3a by axon collaterals of CA3 and CA2 PCs (not all cells) (Fig. 11) creates the hippocampal associative pathway. Contributing CA3 PCs are organized in a reverse gradient to those that give rise to Schaffer collaterals, such that the closer a CA3 PC is to CA2 the more likely it is to contribute to the core element (Lorente de Nó, 1934). I suggest this structure to constitute the core element of the intrinsic oscillator. Such a location of the core element is consistent with the findings that (a) PC discharge is critical for the oscillation, and (b) gap junction-mediated axo-axonic interactions are essential. The full oscillator is formed through the interaction of the active core element with associated axons of interneurones, and their consequent activation. The function of the interneurones is therefore 'secondary'.

The mechanisms underlying oscillatory activity

How do the oscillations work? The cholinergic input serves only as an enabling agent and oscillations depend on the networks synaptic interactions. Activation of the core element by the acetylcholine-mediated reactions of (a) generation of action potentials in CA2 and CA3 PCs and (b) facilitating gap junction-mediated axo-axonic interactions, together with consequent activation

of interneurones, provides the minimal and sufficient conditions for the hippocampal network to adopt the oscillatory mode of activity. The functional consequences of these reactions are the formation of activation pathways (responsible for the individual patterns), and the creation of a reverberatory system (to ensure critical number of action potentials). Pacing is achieved through the probabilistic process of creating and maintaining these activation pathways. In turn, a robust 'clock' is formed, and as long as activation pathways are formed and sufficient number of action potentials are provided, within a safety range, the oscillatory repertoire would be faithfully reproduced. This 'clock' is not of fixed identity, but depends on the activity of the probabilistic core element. Moreover, such a mechanism can function under conditions of low and tightly regulated numbers of action potentials.

The probabilistic formation of activation pathways arises from the fact that gap junctions are not necessarily open continuously during oscillations. This is quite important for the expression of multirhythmicities by the hippocampal network. This probabilistic feature allows the activation of different activation pathways, of similar and dissimilar electrotonic distances, which in turn would determine the frequencies and pattern. Such a process is evident in the oscillatory sequences of all cells, where almost no two consecutive identical cycles are seen, meaning that different activation pathways are activated at different times in a probabilistic manner.

Functional activation of the processing in the axonal compartment, i.e. the core element and associated axons of other cells, during the oscillatory mode of activity forms a probabilistic clock. Formation of the clock is not a result of fixed hardwiring, but of a distributed network (axonal) processing that changes its inter- and intraconnectivity, such that there exists many and different options to reach the same solution, due to the probabilistic and distributed nature of the oscillator. There is no unique solution, but a single global solution (the activation of the distributed and probabilistic oscillator). Thus, a robust clock that faithfully produces the oscillatory mode of activity as long as its activation conditions are met is formed.

The oscillator in action

Not only does such a mechanism account for the phenomena and patterns observed during oscillations, it could also explain some basic features of the oscillatory activity such as why the oscillations are based on a frequency band rather than a single frequency, multirhythmicity and more. Some interesting and difficult to resolve issues are discussed below.

Several of our results are supported and accounted for by such a mechanism. The oscillatory patterns in interneurones, DGCs and CA1 PCs are governed by a synchronized excitatory input (Fischer *et al.* 1999; Fischer *et al.* 2002). In the case of CA1 PCs, oscillatory activity was strongly influenced by the coupling between the oscillator and Schaffer collaterals. As a result of enhancement in gap junction coupling (NH_4Cl experiments) CA1 PCs exhibited excitatory theta oscillations of increased amplitude, while an opposite effects was observed when the inhibitory tone was increased (Fischer & Dürr, 2003), both without affecting either the pattern or the frequency. Within the scope of the presented framework, I interpret the decrease in CA1 PCs' theta amplitude during the increase in inhibitory tone to represent an effect of inhibition to decouple the Schaffer collaterals from the oscillator. In addition, decrease in gap junction-mediated Schaffer collateral–core element coupling can lead to (a) blockade of Schaffer collateral output to CA1 (when inhibitory tone was increased) (Fischer & Dürr, 2003) and (b) the blockade of oscillatory activity when NH_4Cl was removed. Moreover, while excitatory activation pathways account for the oscillatory pattern of interneurones, coupling of interneurones to the core element can account for their discharge activity. Such coupling, through spike transmission, explains how interneurones, and some CA3 PCs, discharge without being depolarized, and how the discharge of interneurones, at the level of individual cells and populations, is synchronized in the phase domain (Fischer & Dürr, 2003). Under control conditions the process of spike transmission from PCs to interneurones is infrequent and depends on excitatory transmission (Miles, 1990; Traub & Miles, 1995; Marshall *et al.* 2002), while during oscillation I assume (within the scope of the presented framework) that this process is enhanced, and additionally occurs through the newly generated pathways of gap junctions. Thus, the postulated gap junction-mediated axonal coupling between pyramidal cells, which constitute the core element, and interneurones may account for a significant part of their activity during oscillations. An additional consequence of spike transmission is the appearance of spikelets. Moreover, as a consequence of interneurone function to dynamically regulate the oscillator (Fischer & Dürr, 2003), I assume (within the scope of the presented framework) that an increase in the inhibitory tone leads to the dilution of the excitatory input to interneurones (Fischer & Dürr, 2003) through a decrease in the availability of activation

pathways. Furthermore, shutdown of the oscillator by acidification of the cytosol (NH_4Cl experiments) strongly supports the involvement of gap junction-mediated interactions in the generation and pacing functions. Lastly, experiments presented in Fig. 12 and accompanying text demonstrate, at least in principle, that the intrinsic oscillator is functionally active and that a reverbatory system is formed, just by satisfying the conditions of cholinergic activation, generation of action potentials and enhancement of gap junction opening in the hippocampal associative pathway – the intrinsic oscillator.

References

Andersen P, Bland HB, Myhrer T & Schwartzkroin PA (1979). Septo-hippocampal pathway necessary for dentate theta production. *Brain Res* **165**, 13–22.

Baimbridge KG & Miller JJ (1982). Immunohistochemical localization of calcium-binding protein in the cerebellum, hippocampal formation and olfactory bulb of the rat. *Brain Res* **245**, 223–229.

Bragin A, Jandó G, Nádasdy Z, Hetke J, Wise K & Buzsáki G (1995). Gamma (40–100 Hz) oscillations in the hippocampus of the behaving rat. *J Neurosci* **15**, 47–60.

Buhl EH & Lübke J (1989). Intracellular lucifer yellow injection in fixed brain slices combined with retrograde tracing, light and electron microscopy. *Neuroscience* **28**, 3–16.

Buzsáki G (2002). Theta oscillations in the hippocampus. *Neuron* **33**, 325–340.

Draguhn A, Traub RD, Schmitz D & Jefferys JG (1998). Electrical coupling underlies high-frequency oscillations in the hippocampus in vitro. *Nature* **394**, 189–192.

Fischer Y & Dürr R (2003). Inhibitory control of intrinsic hippocampal oscillations? *Brain Res* **982**, 79–91.

Fischer Y, Gähwiler BH & Thompson SM (1999). Activation of intrinsic hippocampal theta oscillations by acetylcholine in rat septo-hippocampal cocultures. *J Physiol* **519**, 405–413.

Fischer Y, Wittner L, Freund TF & Gähwiler BH (2002). Simultaneous activation of gamma and theta network oscillations in rat hippocampal slice cultures. *J Physiol* **539**, 857–868.

Freund TF & Buzsáki G (1996). Interneurons of the hippocampus. *Hippocampus* **6**, 347–470.

Frotscher M & Léránth C (1985). Cholinergic innervation of the rat hippocampus as revealed by choline acetyltransferase immunocytochemistry: a combined light and electron microscopy study. *J Comp Neurol* **239**, 237–246.

Gähwiler BH (1981). Organotypic monolayer cultures of nervous tissue. *J Neurosci Meth* **4**, 329–342.

Gähwiler BH & Brown DA (1985). Functional innervation of cultured hippocampal neurones by cholinergic afferents from co-cultured septal explants. *Nature* **313**, 577–579.

Gähwiler BH, Thompson SM, McKinney RA, Debanne D & Robertson RT (1998). Organotypic slice cultures of neuronal tissue. In *Culturing Nerve Cells*, ed. Banker, G &.Goslin, K, pp. 461–498. MIT Press, Cambridge, MA, USA.

Gray JA (1971). Medial septal lesions, hippocampal theta rhythm and control of vibrissal movement in freely moving rat. *Electroencephal Clin Neurophysiol* **30**, 189–197.

Hirase H, Leinekugel X, Czurkó A, Csicsvari J & Buzsáki G (2001). Firing rates of hippocampal neurons are preserved during subsequent sleep episodes and modified by novel awake experience. *Proc Natl Acad Sci U S A* **98**, 9386–9390.

Johnston MF, Simon SA & Ramon F (1980). Interaction of anaesthetics with electrical synapses. *Nature* **286**, 498–500.

Jung R & Kornmüller AE (1938). Eine methodik der ableitung lokalisierter potential schwankungen aus subcorticalen hirngebeiten. *Arch Psychiat Nervenkrankh* **109**, 1–30.

Kocsis B, Bragin A & Buzsáki G (1999). Interdependence of multiple theta generators in the hippocampus: a partial coherence analysis. *J Neurosci* **19**, 6200–6212.

Lee MG, Chrobak JJ, Sik A, Wiley RG & Buzsáki G (1994). Hippocampal theta activity following selective lesion of the septal cholinergic system. *Neuroscience* **62**, 1033–1074.

Leslie J, Nolan MF, Logan SD & Spanswick D (1998). Actions of carbenoxolone on rat sympathetic preganglionic neurones *in vitro*. *J Physiol* **506.P**, 146P.

Lorente de Nó R (1934). Studies on the structure of the cerebral cortex II. Continuation of the study of the ammonic horn. *J Psychol Neurol* **46**, 113–177.

Marshall L, Henze DA, Hirase H, Leinekugel X, Dragoi G & Buzsáki G (2002). Hippocampal pyramidal cell-interneuron spike transmission is frequency dependent and responsible for place modulation of interneuron discharge. *J Neurosci* **22**, RC197.

Miles R (1990). Synaptic excitation of inhibitory cells by single CA3 hippocampal pyramidal cells of the guinea-pig *in vitro*. *J Physiol* **428**, 61–77.

Spray DC, Harris AL & Bennett MV (1981). Gap junctional conductance is a simple and sensitive function of intracellular pH. *Science* **211**, 712–715.

Swanson LW, Wyss JM & Cowan WM (1978). An autoradiographic study of the organization of intrahippocampal association pathways in the rat. *J Comp Neurol* **181**, 681–715.

Tamamaki N, Abe K & Nojyo Y (1988). Three-dimensional analysis of the whole axonal arbors originating from single CA2 pyramidal neurons in the rat hippocampus with the aid of a computer graphic technique. *Brain Res* **452**, 255–272.

Thomas RC (1984). Experimental displacement of intracellular pH and the mechanism of its subsequent recovery. *J Physiol* **354**, 3*P*–22*P*.

Traub RD & Bibbig A (2000). A model of high-frequency ripples in the hippocampus based on synaptic coupling plus axon-axon gap junctions between pyramidal neurons. *J Neurosci* **20**, 2086–2093.

Traub RD, Bibbig A, Fisahn A, Lebeau FE, Whittington MA & Buhl EH (2000). A model of gamma-frequency network oscillations induced in the rat CA3 region by carbachol in vitro. *Eur J Neurosci* **12**, 4093–4106.

Traub RD & Miles R (1995). Pyramidal cell-to-inhibitory cell spike transduction explicable by active dendritic conductances in inhibitory cell. *J Comput Neurosci* **2**, 291–298.

Traub RD, Schmitz D, Jefferys JGR & Draguhn A (1999). High-frequency population oscillations are predicted to occur in hippocampal pyramidal neuronal networks interconnected by axoaxonal gap junctions. *Neuroscience* **92**, 407–426.

Walter WG (1953). *The Living Brain*. W.W. Norton Co., Inc, New York.

Acknowledgements

I gratefully acknowledge the comments of Professor B. H. Gähwiler, Dr M. Mori and Dr N. Savic, and the technical assistance of Dr R. Dürr, L. Heeb, E. Hochreutener, L. Rietschin, and R. Schöb. Supported by the Dr Eric Slack-Gyr and Swiss National Science Foundations. Professor B. H. Gähwiler kindly provided TIMM stained hippocampal slice cultures.